Conducted EMI prediction using different levels of MOSFET models in a multi-physics optimization context

Mohamed Touré[1], **Françoise Paladian**[1], **Mohamed Bensetti**[2], **Florent Robert**[3], **Laurent Dufour**[3]

1. *Institut Pascal, CNRS UMR 6602, Université Clermont Auvergne*
   Campus universitaire des cézeaux, 4 av. Blaise Pascal
   63178 Aubière Cedex, France
   mohamed.toure@efiautomotive.com

2. *GeePs|, Laboratoire Génie électrique et électronique de Paris, CNRS UMR 8507, CentraleSupelec, Univ Paris-Sud, Sorbonne Universités*
   UPMC Univ Paris 06, 3-11 rue Joliot-Curie, Plateau de Moulon
   91192 Gif-sur-Yvette, France

3. *EFi Automotive Service recherche avancée,*
   77 allée des Grandes combes, 01708 Beynost, France

ABSTRACT. *This paper proposes a modeling methodology for the prediction of conducted EMI in the context of multi-physics optimization. The study of the well-known DC-DC buck converter is chosen as illustration to validate this procedure. A bottom-up approach is used to model the entire structure. The modeling of switching cell, passive elements and also Printed Circuit Board (PCB) is presented. Models validation by comparison with experimental results helps to estimate the influence of each model on the accuracy of results.*

RÉSUMÉ. *Cet article propose une méthodologie de modélisation pour la prédiction des perturbations générées par émission conduite dans un contexte d'optimisations multi-physiques. L'étude du convertisseur DC-DC abaisseur buck est choisie comme illustration pour valider cette procédure. Une approche bottom-up permet de modéliser l'ensemble de la structure. La modélisation de la cellule de commutation, des éléments passifs et aussi du PCB est présentée. La comparaison des résultats de simulation par rapport aux résultats expérimentaux permet d'estimer l'influence de chaque modèle sur la précision des résultats.*

KEYWORD: *power converter, EMC, conducted EMI, modeling, PCB.*

MOTS-CLÉS: *convertisseur de puissance, CEM, émission conduite, modélisation, circuit imprimé.*

DOI:10.3166/EJEE.18.425-439

Extended abstract (without number)

☛ Increasing environmental awareness amongst populations and governments has led European legislators to step up the use of new anti-pollution standards. Indeed, road transport accounts for a large share of greenhouse gas emissions responsible for global warming, and pollutant emissions harmful to health. Many technical improvements to the powertrain or vehicle have already been made or are in the works especially on actuating system.

Actuating systems must satisfy various constraints (temperature, mechanical, electronic, EMC etc) and are characterized by strong interaction between different physic phenomena. To enable development and consistent dimensioning of this type of system, we need optimization during design early stage. However, optimization asks for models with a good balance between accuracy and simulation cost. In this framework, this paper proposes a modeling methodology for the prediction of conducted EMI in the context of multi-physics optimization.

The well-known DC-DC buck converter is chosen to validate our modeling procedure. A bottom-up approach is used to model the entire structure. The modeling of switching cell, passive elements and also Printed Circuit Board (PCB) is presented in the range 150kHz-108MHz. Models validation by comparison with experimental results helps to estimate the influence of each model on the accuracy of results.

1. Introduction

Electromagnetic Compatibility (EMC) performance of a system can be assessed according to standards which specify the maximum allowed level of conducted and radiated disturbances produced by an electronic system. The standard CISPR25 (Commission, 2008) has guided this work that focuses only on compliance with conducted emission levels in the frequency range 150 kHz-108 MHz.

EMC is still too often considered as one of the last phases of product development. However, if integrated in the design phase, the *a priori* estimation of disturbances by simulations can allow a considerable economical gain while shortening the duration of development phases. In this regard, the development of accurate and efficient predictive models that allow the designer to bypass some prototyping phases is necessary. This may require the use of multi-physics optimization if the simulation time of these models are compatible with industrial timelines.

The case of a buck power converter, presented in Section 2, is chosen as an illustrative application example to highlight our method. The modeling approach for each sub parts of this converter is studied in Section 3. Section 4 shows the

comparison between measurement and simulation results and assesses the influence of various level of complexity in the system modeling.

2. Application: buck converter

A validation of our approach is provided through the study of a buck converter, shown in Figure 1, implemented on a Printed Circuit Board (PCB). This application is suitable for our investigations since it involves only one switching cell.

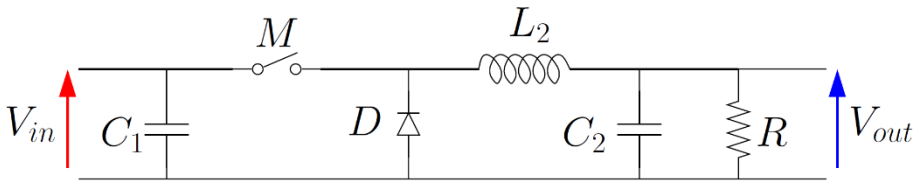

Figure 1. Topology of buck converter

The capacitor C_1 limits the voltage ripples in the converter input. The coil L_2 and capacitor C_2 are used to smooth respectively the current and the voltage on the load R. The switch M and the diode D form the switching cell. In our case, the power switch M is a MOSFET (IPB147N03L) suitable for the current and voltage characteristics of the converter. The diode D is called freewheeling diode. Its role is to ensure the continuity of the current's flow in L_2 at the opening of M. In our study, the freewheeling diode is the internal diode of a MOSFET with the same reference as the controlled switch, which gate and source are short-circuited. The assembled buck converter is shown in Figure 2.

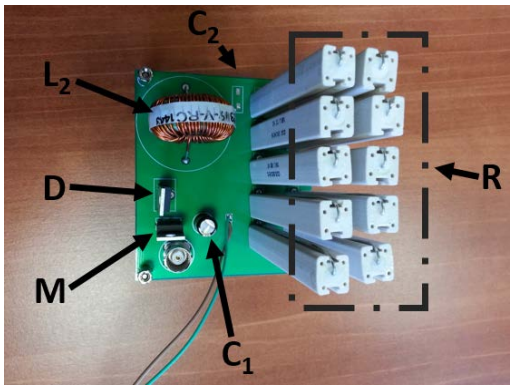

Figure 2. Assembled buck converter

This converter provides an output voltage corresponding to a percentage of the input voltage. This percentage matches with the duty cycle α of M control signal (Rashid, 2010) as shown in Equation (1).

$$V_{out} = \alpha V_{in} \quad (1)$$

The input voltage is set to 10 V, the switching frequency is 200 kHz, and the duty cycle is set to 0.5. This converter is designed with a high inductance L_2 = 390µH and a low resistance R = 1.5Ω on its output to be linked to the impedance of a DC motor and get a similar level of current. The capacitors C_1 and C_2 have a value of 220µF.

3. Model of converter and measuring equipment

A bottom-up approach (Revol *et al.*, 2011) is chosen to model the whole converter based on the modeling of various basic components of the system. We are interested in time-domain modeling to develop a broadband SPICE model of the studied converter taking the measuring equipment into account. Moreover, time-domain modeling helps in considering the non-linearity of the system. On top of that, knowing the time-domain waveforms it would be possible to deduce the frequency-domain waveforms. However, the frequency-domain modeling falls outside the scope of this paper.

First, a time-domain calculation of the circuit waveforms is performed. Then, the frequency spectrum of these quantities is deduced from a FFT. The range of interest's highest frequency sets the maximum time step (Frantz *et al.*, 2013). Since the highest frequency allowed by the standard is 108 MHz, the maximum time step is set to 4.63ns.

3.1. PCB modeling

3.1.1. Overview of the considered setting

The studied converter operates on a PCB. Figure 3 illustrates the PCB layout considered in the modeling of the system.

3.1.2. Choice of trace's model and assumptions

In order to build High Frequency (HF) models of the PCB traces, the circuit is divided into interconnected sub-parts. Each sub-part is considered as a lumped circuit within the frequency range of interest. Therefore, the traces on the PCB are considered as a collection of circuits characterized by their per-unit-length parameters (*L'C'*). Those values depend on both geometrical and electrical parameters of the studied PCB. The per-unit-length resistance and conductance are neglected. Per-unit-length parameters of the PCB traces are shown in Figure 4.

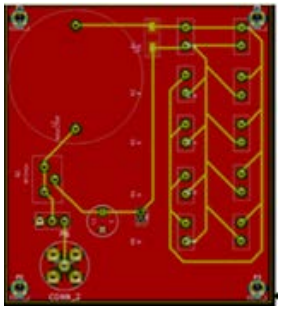

Figure 3. PCB layout of the studied converter

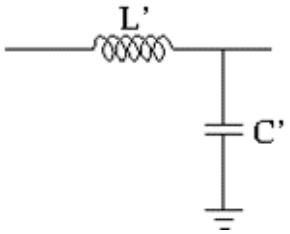

Figure 4. Per-unit-length parameters of PCB trace

The largest length of trace is L_{max}=74.45mm. The maximum frequency considered in this work is 108MHz. Thus, according to the minimum wavelength (λ_{min}=2.7778 m), the traces behave as a lumped circuit. Thus, one cell (*LC*) will allow us to represent each trace. For this study, we assume that the non-linear nature (presence of several knees) on the traces does not influence the transmission behavior up to a few gigahertz (Lafon, 2011). In the context of this work, to see the influence of the PCB taken into account in our SPICE models, the calculations of the per-unit-length parameters are made without any frequency dependence.

3.1.3. Model description

For the modeling of the traces, we assumed the lines to be uniform across the PCB. First, the per-unit-length parameters are computed for a single-cross section of trace. The specific geometry of the studied structure is a microstrip transmission line, as shown in Figure 5.

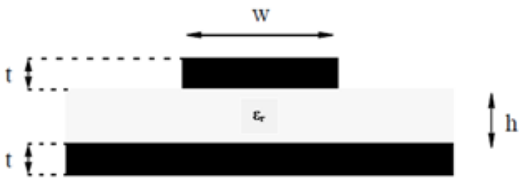

Figure 5. Microstrip structure of PCB traces

Table 1 lists the geometrical dimensions and material parameters of this geometry, including the values of conductivity s of the metal traces and the relative permittivity ε_r.

Table 1. Parameters and dimensions of trace

Dimensions /Parameters	Values
w	0.7 mm
h	1.6 mm
t	35 µm
s	58 MS/m
ε_r	4.26

The per-unit-length parameters are computed using TNT software (Techentin, 2004). Those values are shared in Table 2.

Table 2. Per-unit-length parameters

Per-unit-length parameters	Values
L'	563 nH/m
C'	55.3 pF/m

Multiplying the per-unit-length parameters by the line length enables complete characterization of the traces.

3.2. Active and passive components modeling

3.2.1. MOSFET transistor

The MOSFET as a source of disturbance is the most fundamental element of the circuit. For its modeling, three cases are introduced as listed in Table 3.

Table 3. Different MOSFET models

Cases	MOSFET modeling
n°1	On/off switch MOSFET model
n°2	On/off switch MOSFET model with parasitic elements
n°3	LTspice IV library model

The case n°1 is the most basic form of MOSFET modeling. We have used an on/off model built with a trapezoidal variable resistor $R_{dson/off}$ (Robert, 2015) as shown in Figure 6, where R_{dson} and R_{dsoff} are respectively the MOSFET's on-resistance and off-resistance. R_{dson} value can be inferred from the component datasheet and for R_{dsoff} a large value is chosen like an open circuit, both values are introduced in Table 4.

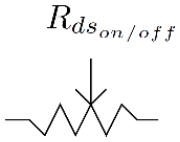

Figure 6. $R_{dson/off}$ MOSFET model

Table 4. MOSFET Rdson/off values

Stray elements	Value
R_{dson}	14.7mΩ
R_{dsoff}	1MΩ

This first model can be improved by adding two parasitic elements: a series inductance L_{ds} and a parallel capacitor C_{ds}. These stray elements help to limit the variation on both, the current flowing through the component and also the voltage at it terminals. Figure 7 depicts this improved model, which is the case n°2. Table 5 presents the values of C_{ds} and L_{ds} which are derived respectively from the MOSFET datasheet and from the MOSFET supplier SPICE netlist.

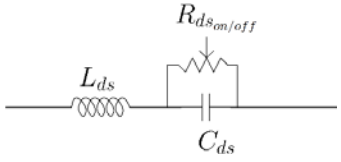

Figure 7. $R_{dson/off}$ with parasitic elements MOSFET model

Table 5. MOSFET stray elements values

Stray elements	Value
C_{ds}	334pF
L_{ds}	3.5nH

A large number of MOSFET models are available in the LTspice IV library (Brocard, 2011). The MOSFET model shared in Figure 8 takes into account the static characteristic, parasitic interconnections (R_G, R_D, R_S), the internal diode (D_{body}), the nonlinearity of the gate-to-drain capacitor C_{DG}, the capacitors C_{GS} and C_{DS}. Figure 8 presents the case n°3.

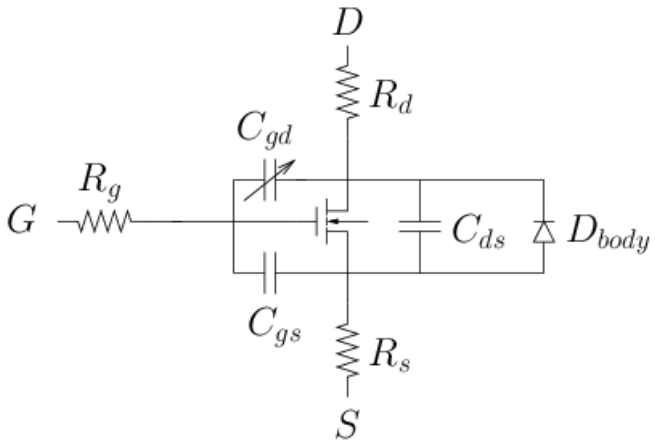

Figure 8. MOSFET model from LTspice IV library

3.2.2. Diode

A static characterization, using a Source Measure Unit (SMU - Tektronix Curve Tracer 370B), can be made to model the diode. Its equivalent SPICE model is developed using Equation (2) to describe its static behavior.

$$I_{forward} = I_S.\left(e^{\frac{V_{forward}}{N.V_t}} - 1\right) \quad (2)$$

$I_{forward}$ and $V_{forward}$ are respectively the current flowing through the diode and the voltage at the diode's ports. N is the emission coefficient and V_t is the thermal voltage. A differential evolution algorithm (Price, 2005) is used to fit these values, which are shared in Table 6. The dynamic behavior of the diode is not taken into account. Figure 9 depicts the good agreement between the model versus the measurement.

Table 6. Diode model coefficient

Coefficient	Value
N	1
V_t	25mV at 25°C
I_s	1^{e-9} A

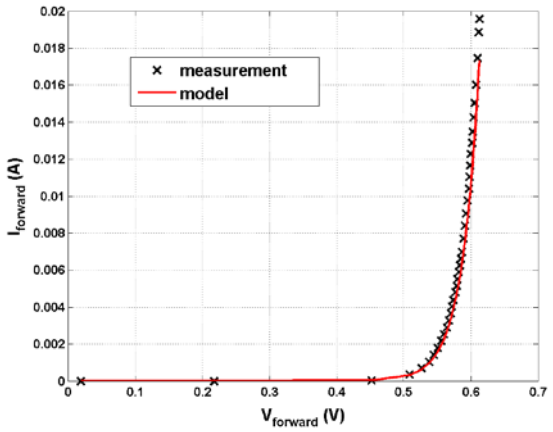

Figure 9. Diode model vs measurement

3.2.3. Passive components

High Frequency (HF) modeling techniques of passive components are widely described in the literature (Pena *et al.*, 2010; Fernández-López *et al.*, 2012; Frikha *et al.*, 2013). In our investigation, HF models are based on measurements performed using a Vector Network Analyzer (Agilent E5071C). The impedance of each component is measured to determine its equivalent circuit in the considered frequency range. Models templates are made up with passive basic network elements like inductors, resistors and capacitors and their specific layout depends on the type of component to be modeled. A differential evolution algorithm (Price, 2005) is used to fit the lumped components values in order to build the equivalent model.

The load resistance model of the studied converter has a capacitive behavior due to the component's interaction at its ports. Therefore, a parallel capacitance of 1 pF is added to the ideal resistance. The connectors have a parasitic inductance of 2.28µH. The resulting load resistance model is shown in Figure 10. Furthermore, Figure 11 presents the good agreement between the load resistance model impedance *versus* its measurement impedance.

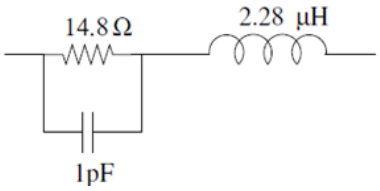

Figure 10. Buck converter load resistance model

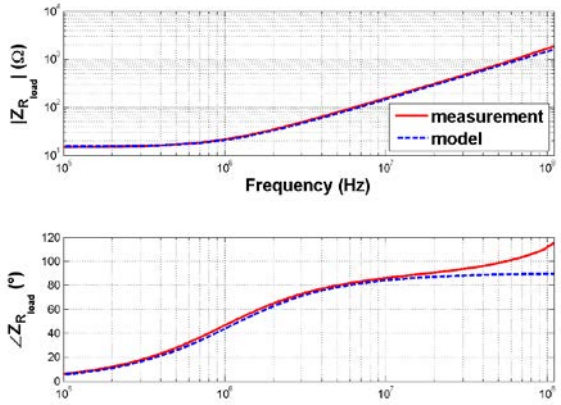

Figure 11. Impedance comparison of load resistance (model vs measurement)

The model of the coil L_2 relies on a perfect inductance with a parasitic series resistor representing the resistance of the winding. The inter-turn electrical couplings are modeled by a parallel capacitance, whereas a parallel resistance characterizes the losses in the magnetic core. Several *RLC* networks are used to represent the different resonances and anti-resonances in high frequency range. The model of the converter output coil L_2 is given in Figure 12. The comparison between the output coil model impedance versus the measurement impedance is depicted in Figure 13. This model is seen to be in good agreement with the measurement.

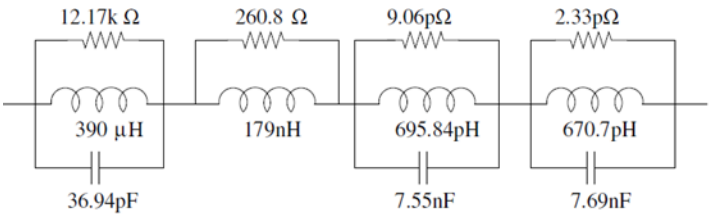

Figure 12. Buck converter output coil model

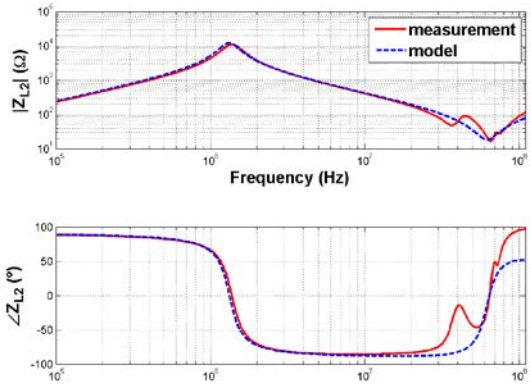

Figure 13. Impedance comparison of the output coil (model vs measurement)

The capacitor models for C_1 and C_2 are based on ideal capacitors with added parasitic effects due to the influence of the connectors introduced as a series resistance and inductance. The resulting models of C_1 and C_2 are shown in Figure 14 and Figure 15 respectively.

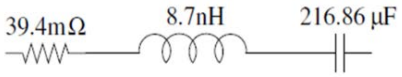

Figure 14. Capacitor C1 model

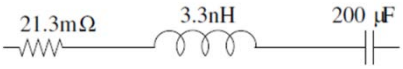

Figure 15. Capacitor C2 model

3.4. Measuring equipment modeling

An accurate modeling of the measuring equipment, including a Line Impedance Stabilization Network (LISN), is required to validate the model by comparison with experimental results. Figure 16 shows the measuring setup set by the standard CISPR25 (Commission, 2008).

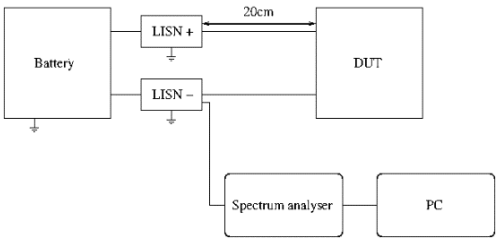

Figure 16. Conducted emission setup

Figure 17 shows the LISN model (Schwartzbeck NNBM 8124), proposed by its manufacturer.

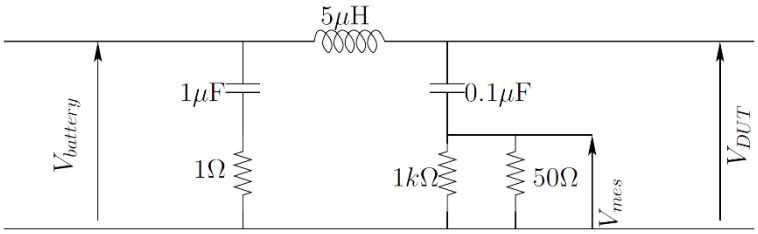

Figure 17. LISN model

4. Comparison between simulation results and measurements

In this section, the different models described in Table 3 are compared to measured data, with the aim to assess their accuracy. The quantity of interest for this comparison is the voltage V_{mes} generated at the LISN + as shown in *Figure 16*. We represent the envelope of simulation results for the various models offered only at the multiple frequencies of the MOSFET switching frequency. Figure 18 presents the comparison between the results envelope for the cases n°1 and n°2.

The MOSFET modeling using only on/off model according to the case n°1 allows prediction of the spectrum up to 10MHz. However, it is clearly demonstrated that adding parasitic elements (case n°2) increases the accuracy of prediction especially above 30MHz. For example, there is a resonance at around 52 MHz in the measured spectrum due to the parasitic inductance of the loop and the parasitic gate-to-source capacitance of the MOSFET. Whereas the model of case n°1 did not correctly predict this resonance, the model of case n°2 leads to estimate this resonance phenomenon at a frequency of around 50 MHz. These results illustrate the importance of correctly modeling the parasitic elements of the MOSFET in this circuit. We introduced in Figure 19 a comparison between cases n°2 and n°3.

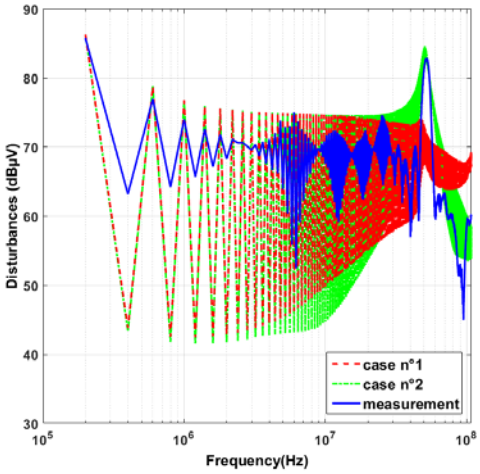

Figure 18. Comparison between case n°1 and case n°2

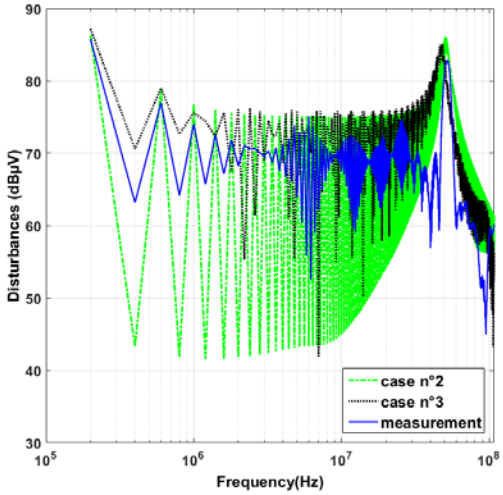

Figure 19. Comparison between case n°2 and case n°3

The MOSFET model issued from LTspice IV library enables a better prediction of the conducted emission spectrum. In fact, the case n°3 provides results with an amplitude slightly higher than measured, which provides a safety margin compared to the experimental results in this application. Figure 20 deals with the comparison between the cases n°1 and n°3.

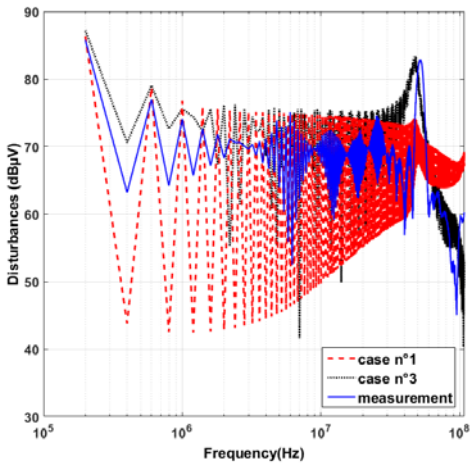

Figure 20. Comparison between case n°1 and case n°3

We note that MOSFET model issued from LTspice IV library permits to characterize the resonance phenomenon around 47 MHz.

The final step of the study matching with system optimization, the model shared through case n°3 seems relevant to the extent that the results are obtained in less than ten minutes using Intel(R) core(TM) i7-4790 CPU @ 3.60GHz.

5. Prospects and conclusions

This paper proposed a modeling approach for conducted EMI on power electronic system applied on a buck converter. Three alternative models with increasing complexity have been compared to measurement in order to validate the theoretical equivalent schemes. In all cases, the proposed PCB and MOSFET modeling approaches provide simulation results that predict the overall behavior of the system regarding conducted EMI, nevertheless with different level of accuracy.

In particular, we noticed the importance of considering the parasitic elements in the model of the MOSFET to achieve more accurate results in the higher frequency range. The multi-physics optimization context requires models for fast simulations. Depending on the final goal, MOSFET modeling with case n°2 or case n°3 could be implemented in a system optimization. In a multi-physics optimization context, the relevance of such an approach is supported by the accuracy of the results got in less than ten minutes.

In future work, we plan to increase the accuracy of MOSFET models by including the voltage dependence of the intrinsic capacitance. Another step of our work consists in modeling the common mode impedance. The model of LISN will be also enhanced by modeling through each of its elements.

Acknowledgements

This work is done in the framework of partnership between the company EFi AUTOMOTIVE, the Labex Imobs3 and the laboratory GeePs.

Bibliography

Frikha A., Bensetti M., Boulzazen H., Duval F. (2013). Influence of PCB and Connections on the Electromagnetic Conducted Emissions for Electric or Hybrid Vehicle Application, *IEEE Transactions on Magnetics*, vol. 49, n° 5, p. 1841-1844.

Pena A., Bensetti M., Duval F., Ravelo B. (2010). Modeling of passive components from the measured S-parameters and application for low-pass filter characterization. *14th International power electronics and motion control conference*, Ohrid, Republic of Macedonia.

Revol B., Roudet J., Schanen J. L. and Loizelet P. (2011). EMI Study of Three-Phase Inverter-Fed Motor Drives, *IEEE Transactions on Industry Applications*, vol. 47, n° 1, p. 223-231.

Brocard G. (2011). *The LTspice IV simulator, manual methods and applications, Würth electronik*: Dunod.

Commission, International Electrotechnical. (2008). CISPR 25: Radio Disturbance Characteristics for the Protection of Receivers Used on Board Vehicles. Boats and on Devices-Limits and Methods of Measurement. Geneva.

Frantz G., Frey D., Schanen J. L., Revol B., Bishnoi H. and Mattavelli P. (2013). EMC models for power electronics: From converter design to system level. *2013 IEEE Energy Conversion Congress and Exposition*, Denver, CO, p. 4247-4252.

Lafon F. (2011). Technics and methodologies development to take into account EMC constraint in Automotive equipment design. Immunity analysis from component until equipment. PhD dissertation. INSA Rennes, France.

Fernández-López P., Bensetti M., Duval F., Vincent G., Baudry D. (2012). Low-impedance passive component modelling using S-parameter measurements. *16e Colloque International et Exposition sur la Compatibilité Electromagnétique (CEM'12)*, Rouen.

Paul C. R. (2008). *Analysis of Multiconductor Transmission Lines*, John Wiley & Sons.

Price K. V. (2005). *Differential Evolution: A Practical Approach to Global Optimization.* Berlin : Springer.

Rashid M. H. (2010). *Power Electronics handbook: Devices, Circuits and Applications.* s.l. : Academic press.

Robert F. (2015). Multiphysic optimization of an electromechanical actuation system. phD dissertation. Centrale Supélec, Gif/Yvette, France.

Techentin B. (2004). *TNT User's Guide.*